**Zeitschrift:** Schweizerische mineralogische und petrographische Mitteilungen =

Bulletin suisse de minéralogie et pétrographie

**Band:** 71 (1991)

Heft: 1

**Artikel:** K-Ar dating of manganese minerals from the Eisenbach region, Black

Forest, southwest Germany

Autor: Segev, Amit / Halicz, Ludwik / Lang, Barbu

**DOI:** https://doi.org/10.5169/seals-54349

## Nutzungsbedingungen

Die ETH-Bibliothek ist die Anbieterin der digitalisierten Zeitschriften auf E-Periodica. Sie besitzt keine Urheberrechte an den Zeitschriften und ist nicht verantwortlich für deren Inhalte. Die Rechte liegen in der Regel bei den Herausgebern beziehungsweise den externen Rechteinhabern. Das Veröffentlichen von Bildern in Print- und Online-Publikationen sowie auf Social Media-Kanälen oder Webseiten ist nur mit vorheriger Genehmigung der Rechteinhaber erlaubt. Mehr erfahren

## **Conditions d'utilisation**

L'ETH Library est le fournisseur des revues numérisées. Elle ne détient aucun droit d'auteur sur les revues et n'est pas responsable de leur contenu. En règle générale, les droits sont détenus par les éditeurs ou les détenteurs de droits externes. La reproduction d'images dans des publications imprimées ou en ligne ainsi que sur des canaux de médias sociaux ou des sites web n'est autorisée qu'avec l'accord préalable des détenteurs des droits. En savoir plus

#### Terms of use

The ETH Library is the provider of the digitised journals. It does not own any copyrights to the journals and is not responsible for their content. The rights usually lie with the publishers or the external rights holders. Publishing images in print and online publications, as well as on social media channels or websites, is only permitted with the prior consent of the rights holders. Find out more

**Download PDF:** 18.10.2025

ETH-Bibliothek Zürich, E-Periodica, https://www.e-periodica.ch

Frau Prof. Dr. Emilie Jäger gewidmet

## K-Ar dating of manganese minerals from the Eisenbach region, Black Forest, southwest Germany

by Amit Segev, Ludwik Halicz, Barbu Lang and Gideon Steinitz<sup>1</sup>

#### **Abstract**

K-bearing manganese minerals from granite-hosted hydrothermal veins in Eisenbach, Black Forest, SW Germany, were used for determining the age of ore emplacement by the K-Ar dating method. The veins in the area are of multiphase origin, filling open fractures and fissures oriented mainly NW, semi-parallel to one of the main fracture zones. They are composed mainly of quartz and barite, with Mn and Fe oxides.

The Mn-ores are composite materials of Mn oxides mixed with syngenetic and/or primary silica minerals from the host-rocks. Therefore, the age of the impure Mn-ore whole-rock differs from the ages of the K-bearing Mn-phases, as it reflects the quantitative proportions of the various components.

The results show that the oldest Mn phase is represented by concentric hollandite and radial, coarse cryptomelane of Permian age ( $> 253 \pm 5$  Ma). A younger phase is represented by massive hollandite and braunite, and banded hollandite, pyrolusite, in places associated with scheelite, yielding Early Cretaceous ages (110–130 Ma).

The latest assemblages consist of massive hollandite, braunite and cryptomelane, massive and crystalline pyrolusite, and hausmannite, coronadite and hollandite, yielding Neogene ages (from about 5 Ma to  $16 \pm 1$  Ma).

The K-Ar dates of Mn minerals demonstrate good correlation of the mineralogenic events with the geochronology of the host-rocks and of the other mineralization products in the area. These results are in accord with the geological setting of the area studied. The Mn phases show a high retentivity of Ar even in situations where earlier phases are in intimate relation with the later ones. Therefore, it can be concluded that the K-bearing Mn-ores are, in principle, datable by the K-Ar method.

Keywords: Geochronology, K-Ar method, manganese ore, Black Forest, Germany.

## Introduction

Direct age determination of ore bodies and/or mineralization phenomena is generally problematic and in many cases impossible, mainly due to the lack of minerals suitable for dating. K-bearing manganese minerals, most of them from the psilomelane-manganomelane group (cryptomelane, hollandite, coronadite, psilomelane), contain K as a minor element in their formulas or as substitution for other cations, and can therefore potentially be used for determining the age of ore emplacement by the K-Ar and Ar-Ar methods. Dating of such minerals, which though to date is still limited, has been preliminarily described by Segev and Steinitz (1986), and Segev et al. (1991).

The present study focusses on granite-hosted manganese veins from the Eisenbach area, Black Forest, southwest Germany (Fig. 1). The geological history of the area is well known. Furthermore, the mineralization history and especially that of the manganese minerals are amply documented. They serve as a basis for the present attempt to examine the K–Ar systematics and the suitability of these minerals for radiometric age determination.

In many cases manganese ores are composite materials in which manganese oxides are generally admixed with syngenetic and/or primary silica minerals (relics from the host-rock). Dates obtained for the manganese ore per se may significantly differ from the true ages of the manganese phases, and may just reflect the proportion of the

<sup>&</sup>lt;sup>1</sup> Geological Survey of Israel, 30 Malkhe Yisrael St., Jerusalem 95 501.

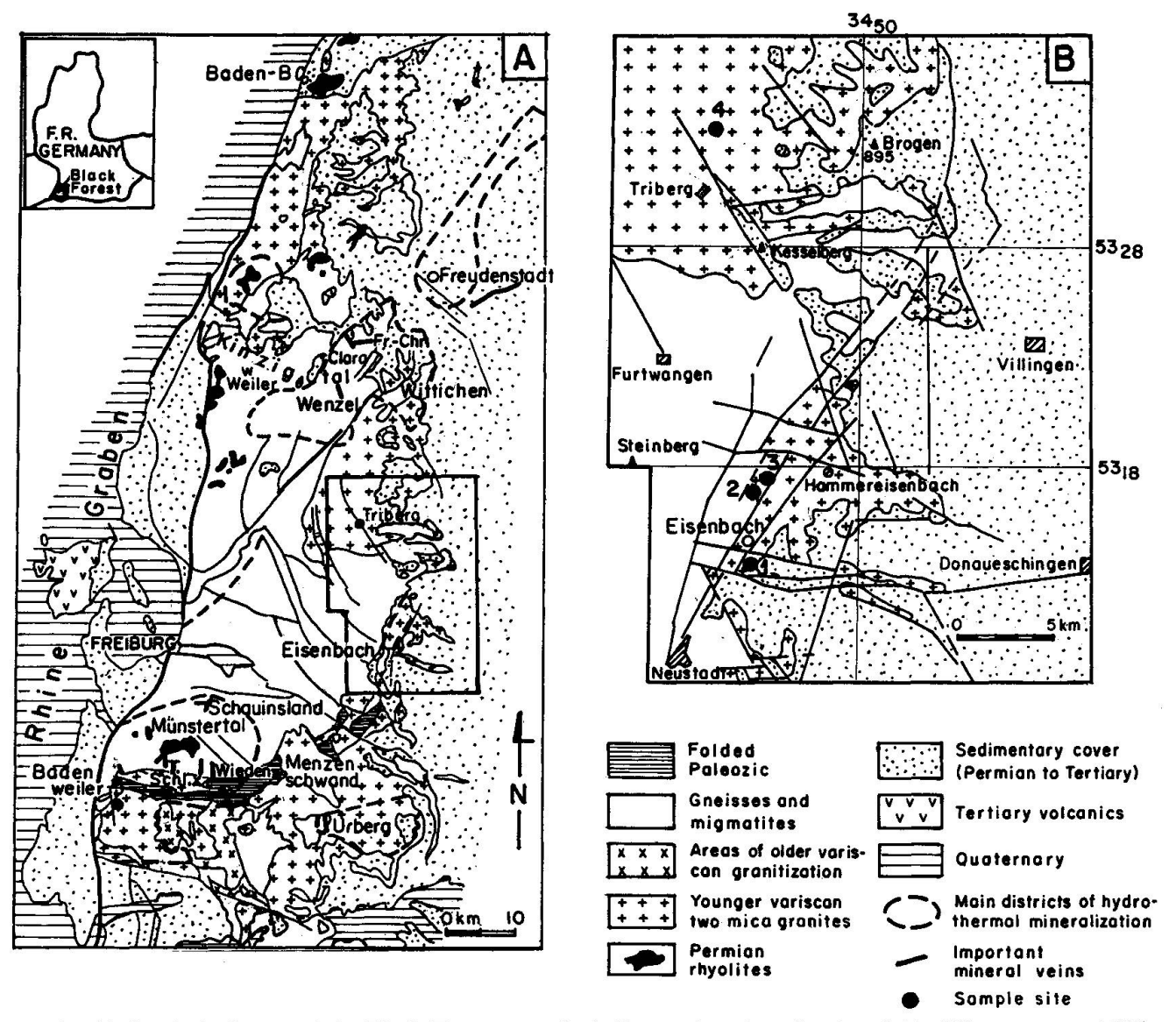


Fig. 1 A) Geological map of the Black Forest area, including main mineralization fields (WIMMENAUER, 1980). B) Enlarged area with the location of the studied sites.

various components. Therefore, in order to determine the K-Ar ages of the pure manganese oxide phases a specific analytical procedure was developed and utilized.

## Geological background

Vast granite intrusions were emplaced in the Black Forest region during the Hercynian orogeny in the interval roughly ranging from 370 to 310 Ma ago (Fig. 2; Working Group Geochronology, 1985). The manganese veins in the Eisenbach region (central Black Forest) under discussion are hosted mainly in the Eisenbacher two-mica granite. This granite belongs to the "young intrusions" phase, around 325 Ma (Wendt et al., 1970; Leutwein and Sonet, 1974);

according to Working Group Geochronology (1985) this phase probably ended about 310 Ma ago (for the southern Black Forest about 20 Ma earlier (Lippolt et al., 1983). Following this plutonic phase, the area was uplifted by horst-and-graben tectonics associated with 310–280 Ma old clastics and calc-alkaline volcanics of predominately acid to intermediate composition (Lippolt et al., 1983). Red beds which covered the area during the Lower Triassic time (Buntsandstein; Herrmann, 1962), about 245 Ma ago, were stripped during the Tertiary uplift which is associated with the Rhinegraben fracturing and volcanic activities.

Arcogenesis (a tectonomagmatic platform activity with vertically accentuated dynamics of crust and mantle) processes from the Upper Carboniferous to the end of the Cretaceous may possibly have

played a role in the structural development and endogenous as well as exogenous formation of deposits (Baumann et al., 1985).

Several volcanic phases have been recorded from the Upper Cretaceous (25 km to the west, near Freiburg and at Hochkopf some 30 km to the southwest) through the Neogene. The younger volcanic events were recorded from Kaiserstuhl (around 16–18 Ma) some 40 km to the west and from Hegau (8 Ma) some 40 km southwest of Eisenbach (HORN et al., 1972).

Several stages of metallogenesis are recognized in the Hercynian massifs in central Europe. Based on fluid inclusion studies, Thomas and Tischendorf (1987) concluded that the pegmatitic-high temperature hydrothermal characteristics of the first Hercynian magmatic-metallogenetic stage in the Erzgebirge and Vogtland are due to high heat flow connected to intensive, short-duration endogenic processes. A second hydrothermal stage was characterized by decreasing heat flow and long term extensive processes. They also suggest that in the Cretaceous the heat flow increased again. A magmatic-metallogenetic stage in the Tertiary is considered to have been autonomously activated by an ensimatic-riftogenic regime.

In the last twenty years efforts have been made to date the various mineralization phenomena in the Hercynian massifs in central Europe by radiometric methods (reviewed, among others, by Bonhomme et al., 1983; Lippolt, 1984; the Working Group Geochronology, 1985; von Gehlen 1987; Dill, 1988), which have led to the following chronometric framework:

U/Pb ages of pitchblendes from Hercynian massifs in southern Germany yield dates ranging between 310 and 280 Ma ago (Wendt et al., 1979; Carl and Dill, 1984). Sm-Nd dates of 298 ± 23 and 281 ± 23 Ma were measured on fluorite which replaced the pitchblende (Leipziger, 1986). K-feldspar which is associated with this fluorite in the same vein yielded a Rb-Sr date of 264 ± 4 Ma (Lippolt et al., 1985).

U-Pb dates of pitchblendes from the Bohemian Massif (Bernard and Legierski, 1975) show a wide spread, between 220 and 150 Ma, and a well-defined peak between 280 and 260 Ma. Other U-Pb measurements of Wittichen pitchblendes yielded Lower Cretaceous ages (Kirchheimer, 1957).

A few dates of mineralization events in the Black Forest were determined by the K-Ar, Ar-Ar and Rb-Sr methods on minerals associated with the metallic mineralization, such as muscovite, adularia, sericite and illite, all assumed to be contemporaneous with the mineralization. Most of the results reflect a wide range of dates, between 250 and 150 Ma.

The various geochronological studies suggest several mineralization periods (Fig. 2):

- 1) The Carboniferous stage (± 325–285 Ma) pneumatolytic and high temperature hydrothermal mineralization.
- 2) The Permian (Rotliegendes) stage (280–260 Ma) initial peak of a long duration hydrothermal activity.
- 3) The Triassic-Jurassic stage long duration pulsating low temperature mineralization, which is actually a continuation of the previous phase.
- 4) The Cretaceous stage (around 100 Ma) probably of higher temperature relative to the former stage.
- 5) The Tertiary stage renewed higher temperature magmatic-metallogenetic activity.

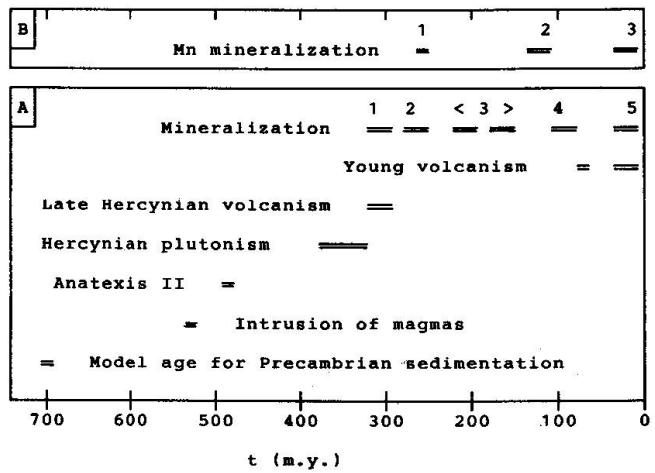


Fig. 2 A) Age of various mineralizations and geological events in the basement of the Black Forest and adjacent areas, based on isotopic studies (after Working Group Geochronology, 1985; Lippolt, 1984; Bernard and Legierski, 1975; Thomas and Tischendorf, 1987). B) Age of the manganese mineralizations as obtained in this study: 1 – concentric hollandite and radial cryptomelane; 2 – massive hollandite and pyrolusite associated with scheelite and silica minerals; 3 – patch-like mixture of cryptomelane, braunite and hollandite; mosaic hausmannite, coronadite and hollandite; braunite with pyrolusite.

The mineralized veins in the Eisenbach region are of multi-phase hydrothermal origin, filling open cross-cutting fissures and fractures striking mainly northwestward, semi-parallel to the Oberbrander fracture zone. They are composed mainly of quartz and barite associated with iron and manganese oxides (Faisi, 1951).

From field, mineralogical and petrographical investigations FAISI (1951) concluded that the hydrothermal activity was composed of two main stages and two additional younger minor phases. The first stage contains early quartz, barite and

hematite followed by psilomelane (I and Ia of Faisi) and pyrolusite. The second main stage includes late hematite, psilomelane (II, IIa) and hausmannite. Faisi (1951) related these assemblages to the Permian tectonic activity (mylonitization and displacements) which followed the Late Hercynian volcanism (mineralization stage 2; Fig. 2). The younger minor stage took place during the Upper Buntsandstein (mineralization stage 3; Fig. 2) and consists of (higher temperature) barite, fluorite and hematite associated with a manganese assemblage of braunite-psilomelane-pyrolusite with some chalcocite and galena. A later secondary mineralization of psilomelane-pyrolusite and wad, with various metallic oxides terminates the metallogenic manganiferous activity in the area.

In his structural analysis, FAISI (1951, Fig. 27) showed that the Buntsandstein is cut by both major fracture zones in the study area (Oberbrander and Eisenbacher fracture zones). This implies intensive post-Triassic movements which may have bearing on the timing of some of the mineralized veins.

## Methods

## SAMPLING AND SAMPLE PREPARATION

The samples were collected at four sites in the Eisenbach and Triberg regions (Fig. 1). Most of the material (samples 1 to 9) came from the Rappenloch underground mine, south of Eisenbach. All the samples are stored in the Geologisches Landesamt of Baden-Württemberg in Freiburg.

To select the K-bearing manganese ores, as well as to study their mineralogy and petrography, each sample was examined in detail, particularly for the content of potassium in the various manganese phases, using SEM (Jeol 840 equipped with a 10,000 Link EDS detector).

Samples in which mineralogical Mn-phases could be distinguished were cut along the contact between the different phases (Figs 3a, 3c). The manganese ore obtained was slightly ground in an agate mortar, sieved, cleaned and further separated from nonmagnetic impurities by a magnetic separator.

In order to study the silicate inclusions separately, selective dissolution of manganese ore was accomplished by: (a) 1:1 HCl at 60 °C (hot water bath) treatment until complete disappearance of black material (4 to 24 hours); (b) separation of the leachate by centrifugation and washing the insoluble residue until complete disappearance of HCl (tested using AgNO<sub>3</sub> as indicator). This process does not affect the Ar retention of the silicate residue to the extent that the K-Ar age of the sample

would be changed, as demonstrated also by Thompson and Hower (1973), Aronson and Douthfitt (1986) and our unpublished experiments on treated illites within Mn nodules as compared with untreated illites from their host-rocks.

A relatively large amount of material was used (a few tens of grams) in order to improve the precision of K determination in the insoluble residue (IR) and to obtain enough IR material for the following potassium and argon determinations.

#### ANALYTICAL PROCEDURES

The mineralogical compositions of the manganese ore and of the insoluble residue were determined by optical microscopy, X-ray diffraction and SEM (Tab. 1).

Major and some trace elements (Tab. 2) were analysed by X-ray fluorescence (Siemens SRS 303) and by atomic absorption spectroscopy (Perkin Elmer 603).

Potassium, for the K-Ar age determinations, was analysed utilizing the following procedure: (1) 250 mg sample dissolved in 15 ml HF + 5 ml HNO<sub>3</sub> (conc.) and evaporated to dryness; (2) 5 ml 1:1 HCl added and evaporated to dryness; (3) 5 ml 1:1 HClO<sub>4</sub> added and heated to a white fume; (4) 5 ml HClO<sub>4</sub> + hot water added to a volume of 500 ml; 1000 ppm Cs added. The amount of K was then determined by atomic absorption spectroscopy (Varian Spectra AA 400).

The Ar analyses (MM-1200 B masspectrometer; Tab. 3) were carried out by the standard isotope dilution procedure in the Geochronological Laboratory of the Geological Survey of Israel. After the extraction and scrubbing of the Ar from the samples, the Ar was trapped on a liquid N<sub>2</sub> cooled charcoal finger and the high vacuum extraction line was pumped briefly to remove considerable amounts of helium due to the decay of uranium present in the Mn-ore.

The error is assumed to be  $\pm$  3% for the K determination,  $\pm$  2–5% for the determination of the amount of IR and  $\pm$  2% for the Ar isotope ratio determinations. Additional error might have been introduced during the selective dissolution, namely, through effects on the potassium and/or argon content of the insoluble residue.

In order to calculate the age of the pure Mnoxide phases, the contributions of the insoluble clays, quartz and feldspar inclusions must be subtracted from the whole-manganese ore dates. The calculation was made using the following material balance equation:

$$T_{Mn} = \frac{(T_{WR} \cdot K_{WR} \cdot 100 - T_{IR} \cdot X_{IR} \cdot K_{IR})}{(K_{WR} \cdot 100 - X_{IR} \cdot K_{IR})}$$

Sample	Location		Manganese minerals						Other minerals					
		руг	bra	hol	crp	cor	hau	qtz	kf	<u>il</u> 1	W	sc	ba	gl
1a	Rappen (1	)		+	0	tr					+			30
1a <sub>IR</sub>	· · · · · ·							1						
1b	11			+	+						+			
1b IR								ŀ						
2	91	٥	0	+	0							tr		tr
2 <sub>IR</sub>	to the state of th									0	+		tı	•
4a	31	+	0	0								0		
4aIR		1							+	0	+			
4b	11	s	0	0				+	0					
4bIR		1						+	0	0	tr			
9	11	1	+	0					tr			tr	•	
9 <sub>IR</sub>									+	0				
10	Sommer (2)	tr	+	0	+				tr					
10 <sub>IR</sub>									+	0				
12	Fahlen (3)		tr	0		0	+				+			
12 <sub>IR</sub>														
14	Gremm (4)	0	+					0						
14 <sub>IR</sub>								+	0	0				

Tab. 1 Location and mineral assemblages of the manganese ore samples from the Black Forest, SW Germany.

- (1) Rappenloch, Coord. R 34<sub>454</sub>/H 53<sub>133</sub>; veins direction 300°–330°.
- (2) Sommerberg, Coord. R 34<sub>454</sub>/H 53<sub>172</sub>; veins direction 300°.
- (3) Fahlenbach, Coord. R 34<sub>462</sub>/H 53<sub>176</sub>; veins direction 300°–310°.
- (4) Gremmelsbach (NE Triberg), Oberotenbach.
- IR Insoluble Residue.

ba	-	barite	ill	– illite	+	<ul> <li>major phase</li> </ul>
bra	<del></del>	braunite	kf	<ul><li>K-feldspar</li></ul>	o	<ul> <li>minor phase</li> </ul>
cor	<u></u>	coronadite	pyr	– pyrolusite	tr	<ul> <li>trace amounts</li> </ul>
crp	_	cryptomelane	qtz	– quartz	(IR)	<ul> <li>insoluble residue</li> </ul>
gl	_	galena	sc	<ul><li>scheelite</li></ul>		
hau	-	hausmannite	W	<ul> <li>− (WO<sub>4</sub>) O<sub>x</sub> precipitated during</li> </ul>		
hol	-	hollandite		<ul> <li>dissolution with 1:1 HCl.</li> </ul>		

where T represents the age (in Ma) as obtained by the K-Ar method for the fractions: WR – whole manganese ore; IR – insoluble residues; and (as calculated) Mn for the manganese oxides. K represents, respectively, the potassium content (in weight percent).  $X_{IR}$  is the weight percent of the insoluble residue.

The maximum cumulative analytical error in this procedure is estimated to be 15%. A higher error was recorded for samples including very low potassium Mn-oxides relative to high potassium content in their associated silicates.

## Mineralogy, petrography and geochemistry

The mineralogical and chemical compositions of the manganese ores and their insoluble residue are presented in tables 1 and 2. The hydrothermal manganese ore from the Black Forest is generally characterized by very high content of tungsten (partly within the manganese minerals and the rest as scheelite) and by a very low amount of iron.

## RAPPENLOCH MINE

1. In sample 1 the inner part (Figs 3a, 4) represents the first Mn precipitation which is cut later by younger veins. The outer part of the sample is composed of hollandite of varying chemical composition. Within this zone two separate mineralization sub-stages are recognized: pre- and post fracturing. The petrographic relationships clearly show at least three stages of fracturing and precipitation of Mn minerals as well as penetration of younger manganese minerals (up to 20% volume) into the

*Tab. 2* Chemical composition of manganese ore samples.

#### A) Majors in wt%

Samples	Mn	BaO	SiO <sub>2</sub>	Al <sub>2</sub> O <sub>3</sub>	Fe <sub>2</sub> O <sub>3</sub>	CaO	K <sub>2</sub> O	WO <sub>3</sub>	PbO	CuO
1a	41.9	11.9	0.3	1.1	0.02	0.1	0.24	2.3	1.0	0.2
1b	41.1	11.4	0.3	2.0	n.d.	0.2	0.89	1.7	1.6	0.1
2	50.3	6.1	2.7	2.1	0.1	1.3	0.39	1.2	0.5	0.2
4a	51.1	4.2	7.0	1.9	0.1	2.2	0.33	1.8	0.1	0.3
4b	37.7	6.0	23.7	3.0	1.3	0.8	0.79	1.9	0.1	0.2
9	48.7	7.4	4.6	1.9	0.2	0.4	0.52	1.1	0.1	0.2
10	52.0	3.8	5.4	2.7	0.3	1.3	1.23	0.7	0.1	0.1
12	56.5	3.7	0.6	0.7	0.1	0.3	0.36	1.3	0.6	0.1
14	48.3	2.0	17.9	2.1	0.4	0.3	0.33	0.1	0.02	0.7

B) Traces (in ppm), L.O.I. and IR (in wt%):

Samples	Со	Sr	ט	v	Zn	L.O.I.	Ir (2)
1a	10	2460	190	90	730	6.7	2
1b	15	4180	150	85	1010	6.0	2
2	15	600	50	60	520	8.9	4
4a	15	n.d.	80	75	320	5.3	4
4b	10	40	20	45	280	6.7	31
9	10	n.d.	30	60	390	7.1	2
10	15	110	10	10	380	7.1	3.5
12	10	60	20	110	170	7.4	1
14	10	n.d.	10	90	70	3.1	21

- n.d. below detection limit
- (1) total iron, reported as Fe<sub>2</sub>O<sub>3</sub>
- (2) amount of insoluble residue after dissolution in 1:1 HCl, 60 °C, including (WO<sub>3</sub>)O<sub>x</sub> precipitated during this treatment.

previously deposited ores, with no evident replacement features. All the manganese components within this sample are free of silica minerals. The inner part (hollandite and cryptomelane) contains the highest amount of potassium (0.9–1.9%  $\rm K_2O$ ). The earlier component of the concentric hollandite (area III and IV in Fig. 4) is highly variable (~0.04–0.45%  $\rm K_2O$ ), and the later component (areas V to VIII) is relatively uniform (0.11–0.17%  $\rm K_2O$ ).

2. Sample 2 (Fig. 3b) shows an irregular structure of fragments of the initial stage (Fig. 5), which consists of large radial crystals of cryptomelane (similar to the area II in sample 1 but richer in K content, up to 2.5%) surrounded by massive colloform pyrolusite, braunite and hollandite. The later stage contains scheelite, barite and galena as accessory minerals, whereas small amounts of illite are disseminated within pores and probably also in the manganese minerals. Unfortunately, we could

not physically separate the older from the younger components.

- 3. Sample 4 was cut into two parts: a) massive hollandite and braunite (4b) cut and replace the granitic host-rock (Figs 3c, 6), and thus contain a large (31%) amount of silicates; and b) a younger vein-filled columnar bands of pyrolusite with minor bands of hollandite (4a) and accessory scheelite. In both parts the silicates contain most of the potassium of the whole sample.
- 4. Penecontemporaneous precipitation of braunite and hollandite (Figs 3d, 7) are the principal manganese constituents of sample 9, with minor pyrolusite. A small amount of scheelite is also coeval with the manganese minerals, whereas silicates and unidentified Pb and Sn minerals were found in small pores.

According to the available material studied, the paragenesis of the manganese minerals in the Rappenloch site (samples 1 to 9) is as follows:

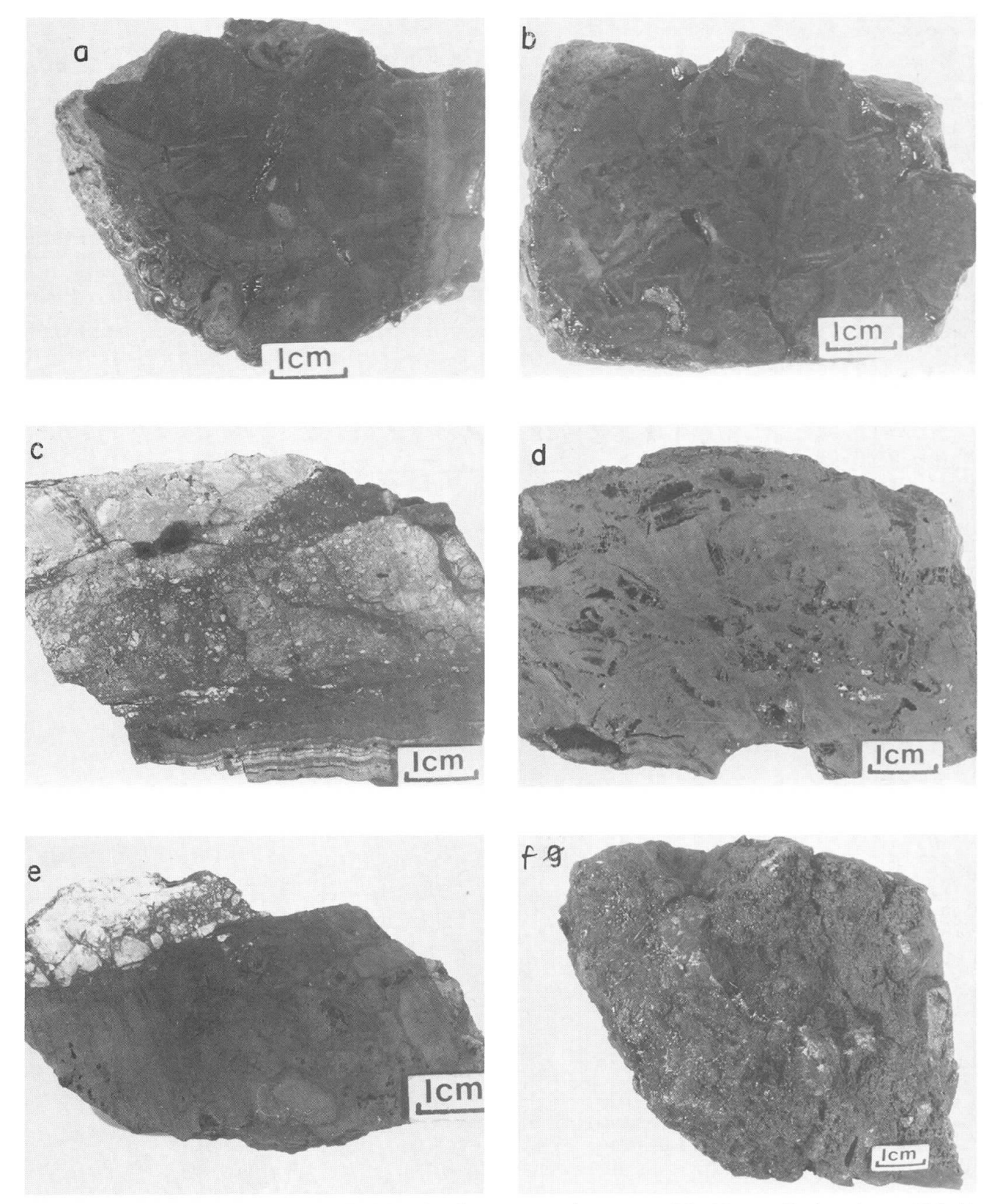


Fig. 3 Photographs of the samples studied showing the macroscopic textures of the Mn-ore (for location see Tab. 1): A) Sample 1 – Concentric outer part (1a), and radial internal part (1b); B) Sample 2 – Brecciated ore with colloform matrix; C) Sample 4 – Vein filling banded ore (bottom, 4a), massive ore (4b), and granite host-rock partially replaced by Mn-oxides (Gr); D) Sample 9 – Pore-filling colloform Mn minerals within massive ore; E. Sample 10 – Cryptomelane-hollandite association, with patch-like texture, at the contact with granite host-rock; F. Sample 14 – Porous pyrolusite-ore.

Tab. 3 K-Ar analytical data.

,		TICAL DA		MEASUR	ED DATES	CALCULATED DATES (Ma)		
Sample	Weight (gr)	K (%)	Ar <sub>RAD</sub> (%)	IR (%)	T <sub>WR</sub>	TIR	$\mathbf{T}_{\mathbf{M}\mathbf{n}}$	T <sub>Mn</sub>
1a	0.341	0.19	27.4	0			117±4	
1a	0.427	0.19	29.4	11		<u> </u>	114±4	
1b	0.051	0.75	71.2	0			255±5	3
1b	0.116	0.75	76.6	"		*	255±5	
1b	0.269	0.75	71.3	"			258±5	
1b	0.244	0.75	69.5	. 11	<u></u>		242±5	
2	0.165	0.33	64.2	4	156±3	İ		
2	0.249	0.33	32.7	91	181±5			
2	0.240	0.33	58.2	"	204±4		27	187±28
2	0.152	0.33	47.3	21	170±4	Anne was that as of-		
2 <sub>IR</sub>	0.078	0.93	19.1	**		106±5		
2 <sub>IR</sub>	0.092	0.93	38.8	71		112±2		
4a	0.269	0.24	54.7	4	98±2			
4a	0.260	0.24	56.7	11	109±2			131±20
$4a_{IR}$	0.093	2.24	44.9	11		55±1		4
4b	0.199	0.66	76.6	30	216±5			
4b	0.228	0.66	75.9	••	199±4			122±18
4b <sub>IR</sub>	0.178	1.70	88.3	11		232±5		
9	0.162	0.41	58.9	2	66±1.5			
9 9	0.044	0.41	47.5	77	70±1			43±6
9	0.281	0.41	27.2	**	119±4			
9	0.254	0.41	18.8	***	81±4			
9 <sub>IR</sub>	0.094	5.79	57.6	71		185±4		
9 <sub>IR</sub>	0.090	5.79	87.7	18		189±4		
10	0.340	0.99	11.0	3.5	17±1.5			
10	0.363	0.99	9.3	99	22±2	8		
10	0.335	0.99	35.5	**	25±0.7			
10	0.215	0.99	26.5	**	20±0.7			7±1
10 <sub>IR</sub>	0.089	2.98	38.1	11		138±4		Secretary Control of the Control of
10 <sub>IR</sub>	0.089	2.98	58.2	11		150±3		
10 <sub>IR</sub>	0.095	2.98	59.4	111		142±3		
12	0.104	0.33	25.4	0			18±1	1 1 1 1 1 1 1 1 1 1 1 1 1 1 1 1 1 1 1
12	0.306	0.33	19.7	11			16±1	
12	0.307	0.33	14.3	11			15±1	
14	0.341	0.28	61.0	21	165±4			
14	0.295	0.28	50.6	11	180±4			7±7
14 <sub>IR</sub>	0.110	1.10	83.7	11		207±4		200,000

### Abbreviations:

 $T_{WR}$  = Ages of Mn-ore including its insoluble silicate minerals

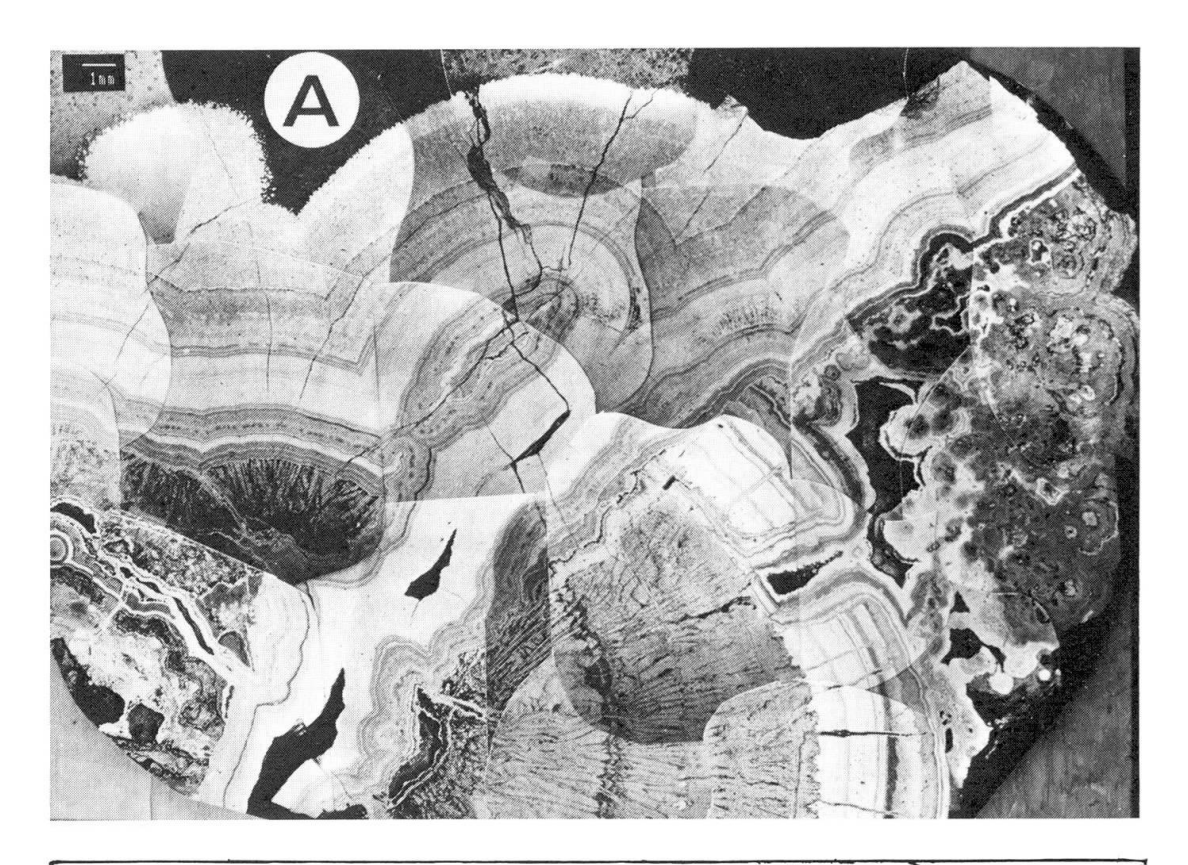
 $T_{Mn}$  = Ages of pure Mn minerals (measured) or of the Mn oxides from samples with silicate contamination (calculated)

 $T_{IR}$  = Ages of insoluble residues from Mn-ores

<sup>1)</sup> The oldest manganese phase is the concentric hollandite + the radial, cryptomelane --> colloform hollandite --> pyrolusite.

<sup>2)</sup> A younger phase is represented by the massive hollandite + massive braunite --> banded pyrolusite + hollandite + scheelite.

<sup>3)</sup> The sequence of massive pyrolusite --> massive braunite contains scheelite, barite, and galena --> hollandite, may belong to the previous phase or may represent a separate younger deposition.



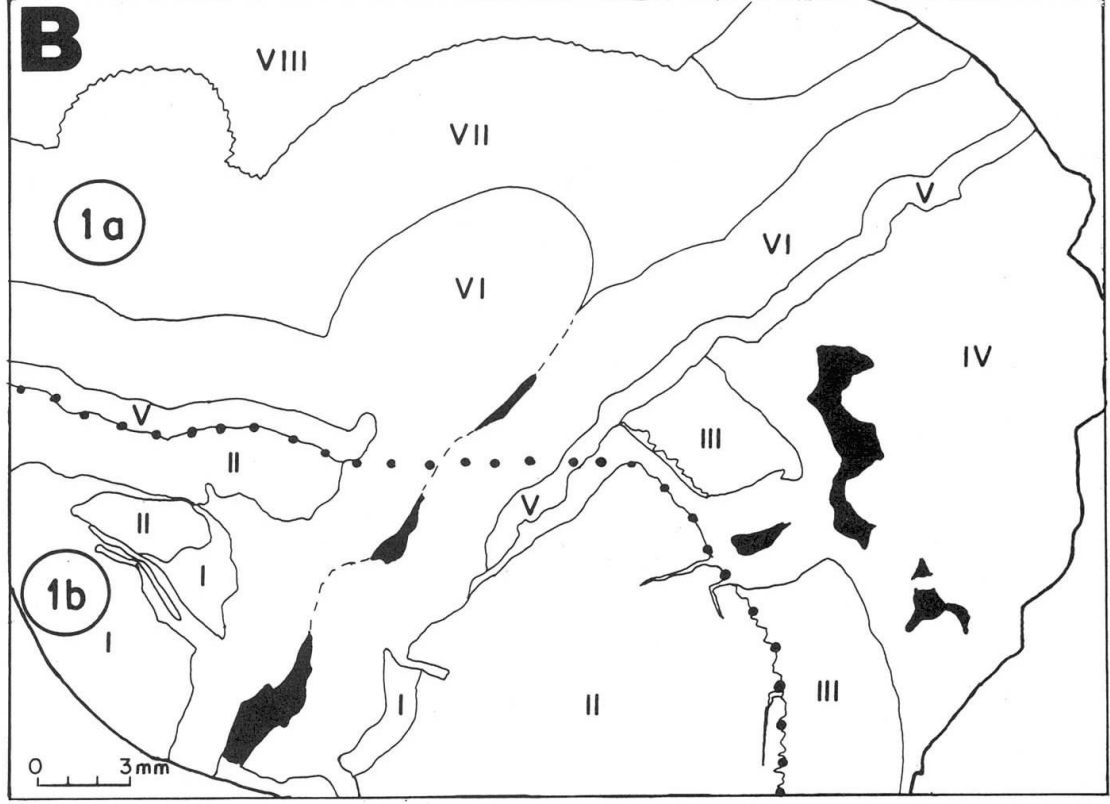
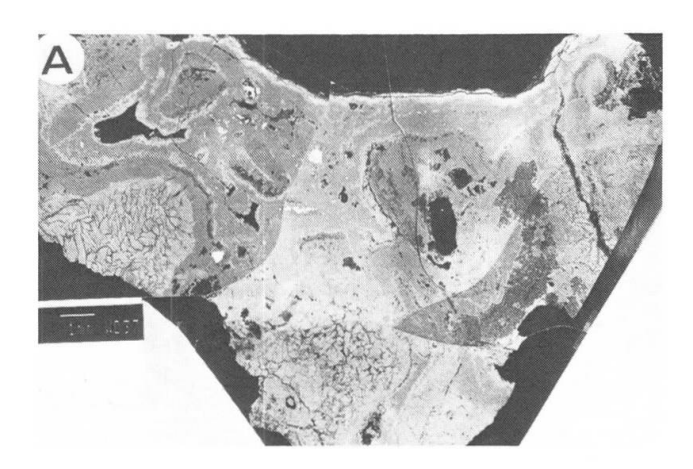


Fig. 4 A) SEM, back-scattered electron-imaging mode (BSE), photomicrograph of sample 1. B) Sketch of 4A. Note the different mineralogic zones: I. concentric hollandite; II. radial coarse cryptomelane showing dark margins due to aluminium-rich pyrolusite and micro-pores; III. banded hollandite; IV. colloform hollandite (hol) and pyrolusite (pyr) penetrating zone III; V–VII. Zones of hollandite of various chemical compositions; VIII. coarse crystallized

pyrolusite. Sample 1a includes zones I–II contaminated by zones V–VI. Sample 1b includes the outer III–VIII zones.

Contact between samples 1a and 1b



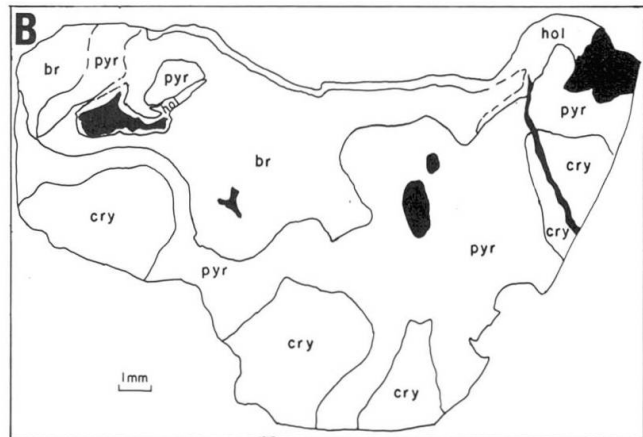


Fig. 5 A) SEM, BSE image, photomicrograph of sample 2. B) Sketch of 5A. Fragments of large radial crystals of cryptomelane (cry), surrounded by a colloform deposition of pyrolusite (pyr), braunite (br) and hollandite (hol). Inclusions of scheelite, barite and galena (white color) are found within the braunite phase.

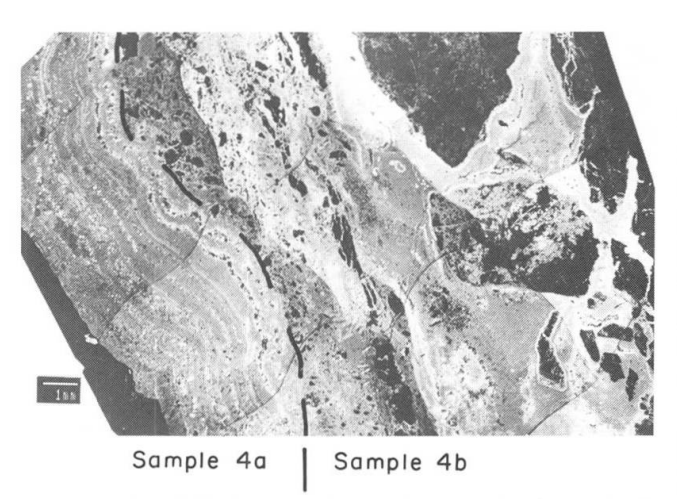


Fig. 6 SEM, BSE image, photomicrograph of sample 4 (dark gray areas) including silica minerals (black areas) cutting through and replacing the granite host-rock (sample 4b). II. Later (sample 4a), vein filling bands of columnar pyrolusite (dark) and hollandite (bright), associated with scheelite (white).



Fig. 7 SEM, BSE image, photomicrograph of sample 9: Penecontemporaneous braunite (br) and hollandite (hol) as principal manganese constituents, with pore-filling colloform hollandite and pyrolusite (pyr).

#### SOMMERBERG-FAHLENBACH

- 1. Sample 10 shows a sharp contact with the highly altered granitic host-rock (Fig. 3e) and is composed of braunite, hollandite and cryptomelane. The intimate intergrowth indicates penecontemporaneous precipitation of the various manganese phases (Fig. 8). The massive cryptocrystalline cryptomelane contains the major amount of potassium in this sample. In addition, small amounts of K-feldspar and illite are disseminated throughout the sample.
- 2. An exclusive mineralogical assemblage of hausmannite + hollandite + coronadite was found in *sample 12* from Fahlenbach. The hausmannite and the coronadite form a mosaic texture (Fig. 9) free of silicates; therefore the potassium is related mainly to the coronadite (recorded also by SEM microanalyses).

## TRIBERG

Sample G-14 consists of a braunite + pyrolusite assemblage which replaced the granite and which therefore contains a high proportion of insoluble residue (21%). As braunite and pyrolusite are poor in potassium, the potassium content (0.28%) must be related mainly to the silica minerals.

In keeping with the above-mentioned observations, the mineralogical and petrographic character of the material studied can be summarized as follows:

- a) The early stages of hollandite and cryptomelane were fractured and displaced, and later used as substrate for younger manganese precipitates
- b) Late mineralization processes have not altered the previously deposited manganese minerals (see samples 1, 2).

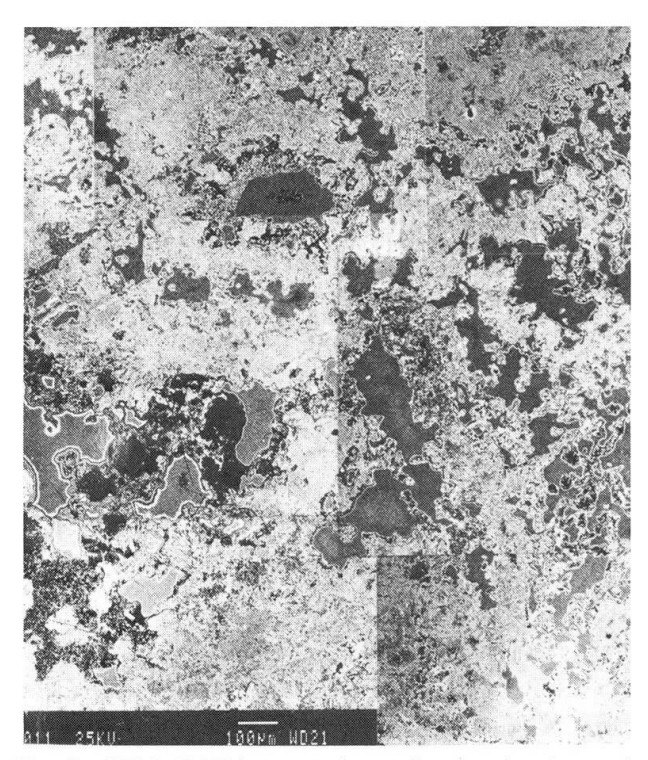


Fig. 8 SEM, BSE image, photomicrograph of sample 10: hollandite and cryptomelane with a penecontemporaneous patch-like texture.

There is agreement between our petrographic observations and the paragenetic sequence suggested by Faisi (1951).

## K-Ar data

The K–Ar age determinations are presented in table 3 in two forms:

- 1. As measured dates i.e., as directly determined on the material analysed, classified according to petrographic type and composition:
  - a) dates of pure K-bearing Mn-oxides  $(T_{Mn})$ .

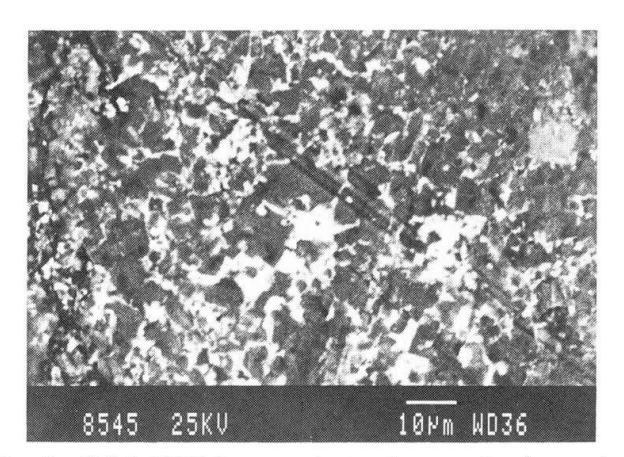


Fig. 9 SEM, BSE image, photomicrograph of sample 12: note hausmannite and coronadite intergrown in a mosaic texture.

- b) dates of mixtures of Mn oxides with silicates  $(T_{WR})$ .
- c) dates of insoluble material within the Mn-ore  $(T_{\rm IR})$ . This insoluble residue may consist of silicates from the host rock as well as syngenetic silicates within the Mn-ore sample.
- 2. As calculated dates for pure Mn-oxide endmembers ( $T_{Mn}$ ). These dates have been calculated from the measured mixture date ( $T_{WR}$ ) and the relevant IR date ( $T_{IR}$ ).

Thus, the age of the K-bearing Mn-ore is derived directly in the case of the pure Mn-phases and indirectly in the cases of the mixtures.

#### MEASURED K-Ar DATA

1. Direct dating of pure Mn mineral phases:

Three dates have been measured for pure Mn phases. The earliest manganese precipitation in Rappenloch (sample 1b) is associated with small amounts of younger, low potassium hollandite. Therefore, the date of  $253 \pm 5$  Ma (Permian) is slightly younger than the true age (minimum age), depending on the amount and the age of the associated younger hollandite (see below).

The pure colloform hollandite deposited in the two parts of the sample 1a (see Fig. 4 a, b, and mineralogical description), yielded a reproducible date of  $116 \pm 4$  Ma (Early Cretaceous). There are two possible interpretations of this date: a) the measured material represents a homogeneous mixture of hollandite from both parts of this sample, whereas each part has a different age; and b) the deposition of the whole colloform hollandite took place in the same time interval.

The youngest pure Mn-oxide phase (sample 12, Fahlenbach) yielded a reproducible age of  $16 \pm 1 \text{ Ma}$  (Neogene).

2. The "whole" Mn ore samples (mixture material):

Meaningless dates, ranging widely between  $207 \pm 5$  Ma (sample 4b) and  $21 \pm 2$  Ma (sample 10), were obtained for the mixtures of Mn-oxides and silicates. The scatter obtained from samples 2 and 10 is attributed to sample inhomogeneities, due to the relatively large grain-size and the small amount of the analysed material.

3. Dating of the insoluble residue (IR) fractions: The dates obtained for the insoluble residues in the Mn-ores cannot be taken as meaningful ages because they consisted, in most cases (4b<sub>IR</sub>; 9<sub>IR</sub>; 10<sub>IR</sub> and 14<sub>IR</sub>), of mixtures between various types of silicates. They also show a wide spread of dates but exhibit good reproducibility in samples with relatively high K content (e.g. samples 9 and 10). An exception to the above is sample 2, in which the

only K-bearing silicate is authigenic illite, which was not observed as a late pore filling phase and is, therefore, assumed to be dispersed within the ore itself. Its age  $-109 \pm 5$  Ma - may, thus, also be meaningful as the age of the Mn minerals.

The date of the IR of sample 4a  $(55 \pm 1 \text{ Ma})$  is much younger than that of the whole ore  $(103 \pm 2 \text{ Ma})$ , indicating that at least part of the silicates in the measured IR were formed after the manganese mineralization itself, probably as a pore-filling phase.

# INDIRECT (CALCULATED) DATING OF THE Mn-OXIDES

Indirect dating of the Mn phase is presented (Tab. 3) for all samples on which whole rock and silicate dates have been obtained.

The calculated Middle Jurassic age of the Mnoxides of sample 2 (187  $\pm$  28 Ma) pertains to the older hollandite/cryptomelane phase in the sample which correlates petrographically with sample 1b. The presence of younger low potassium braunite + hollandite, surrounding the hollandite/cryptomelane phase is probably responsible for the younger calculated age of sample 2 because, the low IR content (4%) with 0.93% K and a mean age of 109  $\pm$  5 Ma does not significantly influence the age determination of the Mn oxides.

Both parts of sample 4 yielded similar calculated Early Cretaceous dates ( $122 \pm 18$  and  $131 \pm 20$  Ma), despite their different chemical and mineralogical compositions. This may be significant as most of the potassium is enclosed in the silicate minerals. Thus, Mn-oxides with low potassium concentrations probably yield meaningful calculated ages. These Early Cretaceous ages of sample 4 are similar (in the range of analytical error) to the age of the pure Mn ore of sample 1a.

In sample 9 the calculated Paleogene age for the manganese oxides  $(43 \pm 6 \text{ Ma})$  is younger than the correlated assemblage of sample 4b but much older than the young phase of sample 12. The age may be explained by the fact that the colloform hollandite surrounds pores in a groundmass of braunite-hollandite. This implies that the groundmass belongs to the Early Cretaceous phase of manganese precipitation, whereas the later colloform phase belongs to the Neogene phase. The  $43 \pm 6 \text{ Ma}$  date may represent a real event, should the above-mentioned mineralogical associations prove to be coeval.

Sample 10, with a relatively high potassium content, which is located within the cryptomelane, has a low silicate content. The calculated Neogene age of the Mn oxides  $(7 \pm 1 \text{ Ma})$  is close to the

whole rock date  $(21 \pm 2 \text{ Ma})$  and can be considered as reliable.

Sample 14 is rich in silicates (21%) which hold most of the overall low amounts of potassium. Therefore, the date of the whole rock (172  $\pm$  4 Ma) is close to that of the IR (206  $\pm$  4 Ma) and the calculated Neogene age for the manganese minerals is very young (7  $\pm$  7 Ma). This age indicates that, similar to samples 12 and 10, the manganese minerals in this sample were formed during the youngest mineralization event. The analytical error is extremely high due to the very low proportion of potassium within the Mn oxides.

#### **Discussion and conclusions**

Argon measurements performed on Mn-ore (ground mostly to  $80\text{--}125~\mu m$  size), exhibit reasonable reproducibility in samples with K > 0.1% and relatively uniform mineralogical composition.

The petrographical observations suggest that the early manganese phases were mechanically fractured and displaced but not altered and/or replaced by later manganese phases; rather the latter are developed as overgrowths on the initial phases or as cavity fillings.

The question concerning the Ar-retentivity of the manganese minerals is of great relevance. In similar K-Ar study of manganese ore from Hungary (K. Balogh, pers. commun.) shows that Mn minerals release their Ar at higher temperature than the coexisting clay material. The good retentivity of the manganese minerals is indicated by the following:

- 1. The K-Ar dates of the Mn minerals, and one of the silica minerals, group to three periods of Mn-mineralization: I. Permian (1b, 2?); II. Early Cretaceous (1a?, 4a, 4b, 9?); and III. Neogene (10, 12, 14). These periods correlate with stages 2, 4 and 5 of the regional mineralization events (Figs 2, 10). Furthermore, the earliest Mn-mineralization belongs to the oldest hydrothermal mineralization period expected in the area (260–280 Ma), whereas the first mineralization stage in the Hercynian massifs (290–310 Ma) occurred under much higher temperature conditions (Thomas and Tischendorf 1987).
- 2. Good correlation exists between the petrographic sequence (Faisi, 1951; this study) and the K-Ar ages (1b and the early precipitates of 2), which paragenetically represent the initial manganese precipitation.
- 3. The intimate relationships of later, newly formed, manganese minerals with the earlier Mn phases does not affect the K-Ar systematics of ei-

ther phase; this, despite the fact that some of the younger phases were probably formed under relatively high temperatures.

- 4. The agreement observed between ages of Mn oxides (such as in 4a, 4b and 1a) and some of the ages of the associated silica minerals, e.g., 2<sub>IR</sub>, reinforces the reliability of the former. Further investigation concerning the identification and dating of different silicates present within the mineral assemblages, however, is required.
- 5. Despite their different mineralogical and chemical compositions, the two parts of sample 4 yielded similar calculated Mn-oxide age.

The first manganese mineralization phase took place during the main phase of the post-Hercynian mineralization period; the second and the third events of manganese formation may possibly be connected with the riftogenic regime in the area studied, which was initiated in the Cretaceous. The latter was associated with intensive volcanism (Horn et al., 1972; WIMMENAUER, 1974 and LIPPOLT, 1982). The calculated Mn-oxide ages of samples 4a, and 4b (131  $\pm$  20 and 122  $\pm$  18 Ma) as well as the measured age of  $2_{IR}$  (109 ± 4 Ma) and possibly the age of sample 1a (around 116 Ma), cannot be attributed to a specific known volcanic event of similar age. The young ages of the manganese ores: e.g., samples  $10 (7 \pm 1 \text{ Ma})$ ,  $12 (16 \pm 1 \text{ Ma})$  and 14 (about7 Ma) are, however, in good agreement with the ages of young volcanics in the close vicinity (Fig. 10).

The fact that the oldest manganese mineralization event, according to this study, took place during the Permian fits well with the interpretation of Faisi (1951), who suggested a pre-Triassic major phase of manganese mineralization. Moreover, the fact that the Triassic Buntsandstein is displaced by the main fracture zones in the study area clearly implies post-Triassic intensive tectonic movements, which can be associated with additional fissure filling hydrothermal manganese mineralization (Cretaceous and Neogene events).

The post Permian hydrothermal manganese mineralization may relate to some of the volcanic events in the Black Forest. These volcanic events could have caused leaching (from available sourcerock), migration and precipitation of manganese and other hydrothermal minerals in the same fracture zones as the previous mineralization.

The intimate assemblages of manganese oxides of different ages (as in sample 1a and 1b, where more than 100 Ma separate between their formation) have implications for understanding depositional processes in similar types of vein filling mineralizations. Greater precision in such cases can be reached by using more advanced dating techniques (e.g. single crystal Ar–Ar determinations).

#### Acknowledgements

The present research was initiated during the stay of the senior author at Heidelberg University and was partially supported by the MINERVA foundation.

We thank Prof. G.C. Amstutz, of Heidelberg University, H. Maus and Derkmann, of the Geologisches Landesamt Baden-Württemberg, Freiburg, and Prof. W. Wimmenauer of Freiburg University, for their kind assistance and for supplying Mn-ore samples from the Black Forest.

C. Dallal, of the Geological Survey of Israel, is acknowledged for his technical help in the argon laboratory, and Beverly Katz, for improving the English language of the manuscript.

#### References

Aronson, J.L. and Douthitt, C.B. (1986): K/Ar systematics of an acid-treated illite/smectite: implication for evaluation age and crystal structure. Clays and Clay Minerals, 34, 4, 473–482.

Baumann, L., Leeder, O. and Weber, W. (1985): The position of platform activation (arcogenesis) and its metallogenetic importance (exemplified by the North Atlantic – West European lithospheric area). In: Wolf, K.H. (ed.) Handbook of strata-bound and stratiform ore deposites. Elsevier, Amsterdam, XII + 529 p. Part IV/12, 409–459.

Bernard, J.H. and Legierski, J. (1975): Position of primary endogenous uraninite mineralization systems of the Bohemian massif. Geol. Surv. Bull. Prague, 50, 321–328

Bonhomme, M.G., Buhmann, D. and Besnus, Y. (1983): Reliability of K-Ar dating of clay and silicifications associated with vein mineralizations in Western Europe. Geol. Rdsch., 72, 105-117.

CARL, C. and Dill, H. (1984): Datierungen an Pechblenden aus dem Nabburg-Woelsendorfer Flussspatrevier. Geol. Jb. D63: 59–76.

DILL, H. (1988): Geologic setting and age relationship of fluorite-barite mineralization in southern Germany with special reference to the Late Paleozoic unconformity. Mineral. Deposita, 23, 16–23.

FAISI, S. (1951): Die Eisen- und Manganerzgänge von Eisenbach (südöstlicher Schwarzwald) und ihre tektonische Stellung. N. Jb. Miner. Abh., 121, 254–271.

tonische Stellung. N. Jb. Miner. Abh., 121, 254–271.
Gehlen, K. von (1987): Formation of Pb–Zn–F-Ba mineralizations in SW Germany: A status report. Fortschr. Miner., 65/1, 87–113.

HERRMANN, A. (1962): Epirogene Bewegungen im germanischen Buntsandsteinbecken und deren Bedeutung für lithostratigraphische Parallelisierungen zwischen Nord- und Süddeutschland. Geol. Jb., 81, 11–72.

HORN, P., LIPPOLT, H.J. and TODT, W. (1972): Kalium-Argon-Altersbestimmungen an tertiären Vulkaniten des Oberrheingrabens I. Gesamtgesteinsalter. Eclogae geol. Helv., 65/1, 131–156.

Kirchheimer, F. (1957): Bericht über das Vorkommen von Uran in Baden-Württemberg. 2, 1–127.

Leipziger, K. (1986): Untersuchungen zur Raumschaffung der Flussspatmineralisationen im Woelsendorfer Flussspatrevier. Ph.D. Thesis, Univ. Mainz, 186 p.

LIPPOLT, H.J. (1982): K/Ar age determinations and the correlation of Tertiary volcanic activity in central Europe. Geol. Jb., D52, 113–135.

LIPPOLT, H.J. (1984): Experimentelle Datierungen von postvaristischen Mineralisationen, Möglichkeiten und Grenzen. In: Sonderdruck aus: Postvaristische Gangmineralisation in Verlag Mitteleuropa, Chemie, Weinheim, 305–359.

Lippolt, H.J., Schleicher, H. and Raczek, I. (1983): Rb-Sr systematics of Permian volcanites in the Schwarzwald (SW Germany) – Part I: space of time

between plutonism and late orogenic volcanism. Contrib. Mineral. Petrol., 84, 272–280.

LIPPOLT, H.J., MERTZ, D.F. and ZIEHR, H. (1985): The late Permian Rb-Sr age of K-feldspar from the Woelsendorf mineralization (Oberpfalz, F.R. Ger-

many). N. Jb. Miner., Mh., 49–57.

Metz, R. (1957): Die Erzführung der Schwarzwald-Randverwerfungen. In: Metz, R., Richter, M. and Schurenberg, H., Die Blei-Zink-Erzgänge des Schwarzwaldes. Geol. Jb., 29, 277.

SEGEV, A. and STEINITZ, G. (1986): Dating of epigenetic manganese nodules and reset illites in the Cambrian Timna Formation, southern Israel. Abstr., Terra Cognita 6, 112–113.

SEGEV, A., STEINITZ, G. and WAUSCHKHUN, A. (1991): Dating of K-bearing manganese minerals - preliminary results. Geol. Surv. Israel Curr. Res., 7, 1–3.

THOMAS, R. and TISCHENDORF, G. (1987): Evolution of Variscan magmatic-metallogenetic processes in the

Erzgebirge according to thermometric investigations. Z. Geol. Wiss. Berlin 15, 1: 25-42.

THOMPSON, G.R. and Hower, J. (1973): An explanation for low radiometric ages from glauconite. Geochim.

Cosmochim. Acta, 37, 1473-1491.

Wendt, I., Lenz, H., Harre, W. and Schoell, M. (1970): Total rock and mineral ages of granites from the southern Schwarzwald, Germany. Eclogae geol. Helv., 63, 365-370.

Wendt, I., Lenz, H., Hoehendorf, A., Bultemann, H. and Bultemann, W.D. (1979): Das Alter der Pechblende der Lagerstätte Menzenschwand, Schwarz-

wald. Z. Dt. Geol. Ges., 130, 619–626.

WIMMENAUER, W. (1974): The alkaline province of central Europe and France. In: SORENSEN, H. (ed.): The alkaline rocks. London, New York, Sydney, Toronto.

WIMMENAUER, W. (1980): The mineral deposits of the Schwarzwald (Black Forest). Erzmetall, 33, 150-152.

Working Group Geochronology (Lippolt et al.) (1985): Isotope geochronology, Schwarzwald. Abstr. 4th Alfred Wegener Conf., Seeheim/Odenwald (96 p.), p. 61, Bonn.

Manuscript received August 23, 1990; revised manuscript accepted December 20, 1990.